Probing the Excitations of a Lieb-Liniger Gas from Weak to Strong Coupling

F. Meinert,[1] M. Panfil,[2] M. J. Mark,[1,3] K. Lauber,[1] J.-S. Caux,[4] and H.-C. Nägerl[1]
[1]Institut für Experimentalphysik und Zentrum für Quantenphysik, Universität Innsbruck, 6020 Innsbruck, Austria
[2]SISSA-International School for Advanced Studies and INFN, Sezione di Trieste, 34136 Trieste, Italy
[3]Institut für Quantenoptik und Quanteninformation, Österreichische Akademie der Wissenschaften, 6020 Innsbruck, Austria
[4]Institute for Theoretical Physics, University of Amsterdam, 1090 GL Amsterdam, Netherlands
(Received 29 May 2015; revised manuscript received 23 July 2015; published 20 August 2015)

We probe the excitation spectrum of an ultracold one-dimensional Bose gas of cesium atoms with a repulsive contact interaction that we tune from the weakly to the strongly interacting regime via a magnetic Feshbach resonance. The dynamical structure factor, experimentally obtained using Bragg spectroscopy, is compared to integrability-based calculations valid at arbitrary interactions and finite temperatures. Our results unequivocally underlie the fact that holelike excitations, which have no counterpart in higher dimensions, actively shape the dynamical response of the gas.

DOI: 10.1103/PhysRevLett.115.085301 PACS numbers: 67.85.-d, 03.75.Dg, 03.75.Gg, 05.30.-d

Interacting quantum systems confined to a one-dimensional (1D) geometry display qualitatively different behavior compared to their higher-dimensional counterparts [1]. Systems of strongly interacting electrons recently realized in electronic nanostructure devices [2,3] have evidenced the breakdown of Landau's Fermi liquid theory of quasiparticles in one dimension, a world in which new types of excitations emerge out of the inevitably collective nature of the dynamics. Understanding these requires approaches that go beyond Landau's paradigm. The best known, valid for sufficiently small temperatures and energies, is the Luttinger liquid (LL) formalism [4]. When probing dynamical correlation functions, however, one typically leaves this low-energy and large-wavelength limit and enters a regime where even recent extensions of the LL formalism to higher energies [5,6] cannot capture all features. Instead, one must rely on nonperturbative calculations to understand the correct basis of excitations and quantitatively explain experiments, a recent example being spinon dynamics in quantum spin chains [7,8]. These systems, however, lack the tunability required to track the whole transformation occurring between the limits of weak and strong coupling.

Very recently, systems of ultracold bosons have opened up new routes to study strong correlation effects in one dimension [9,10]. In particular, tuning the interaction strength [11], as characterized by the dimensionless Lieb-Liniger parameter γ [9], gives access to the full range from weak ($\gamma \lesssim 1$) to strong ($\gamma \gg 1$) interactions and the fermionized Tonks-Girardeau (TG) regime [10–14]. Moreover, the 1D Bose gas with contact interactions is one of the few integrable many-body problems that allows for the combining of experiment with numerically exact studies of the excitation spectrum, making it an ideal setting for observing interaction effects on dynamical correlation functions [15]. In their seminal work [16,17], Lieb and Liniger showed that next to a particlelike mode (Lieb-I mode), which resembles Bogoliubov excitations in the limit of weak interactions, a second mode naturally emerges (Lieb-II mode) that stems from holelike excitations in the effective Fermi sea in one dimension. The coexistence of these two types of elementary excitations leads to a significant broadening of the dynamical response functions, clearly visible in the strongly interacting regime [18,19] (see Fig. 1).

In this Letter, we measure the dynamical structure factor (DSF) of the Lieb-Liniger Bose gas realized with ultracold atoms and confined to 1D quantum tubes. Previous work [15] addressed a fixed intermediate interaction regime ($\gamma \simeq 1$). Here, the tunability of interactions allows us to enter deeply into the strongly interacting TG regime. Our analysis is based on careful disentangling of the experimental traits, and it allows us to identify the role of the Lieb-Liniger dynamics in shaping the response of the system. Comparison of the measured spectra with state-of-the-art numerical calculations [18,20] ranging from the weakly to the strongly interacting regime allows for a clear distinction between interaction and temperature effects and demonstrates the contribution of the Lieb-II type excitations to the response of the system.

Our experiment starts with a cesium Bose-Einstein condensate (BEC) of typically 1.1×10^5 atoms confined in a crossed dipole trap [21,22]. The BEC is adiabatically loaded into an array of ≈4000 quantum wires created via two mutually perpendicular retro-reflected laser beams at a wavelength $\lambda = 1064.5$ nm. At the end of the ramp the lattice depth along the horizontal direction is $V_{x,y} = 30E_R$, creating an ensemble of independent one-dimensional "tubes" with a transversal trap frequency $\omega_\perp = 2\pi \times 14.5$ kHz oriented along the vertical z direction [Fig. 1(a)]. Here, $E_R = h^2/(2m\lambda^2)$ is the photon recoil energy with the mass m of the Cs atom. During lattice

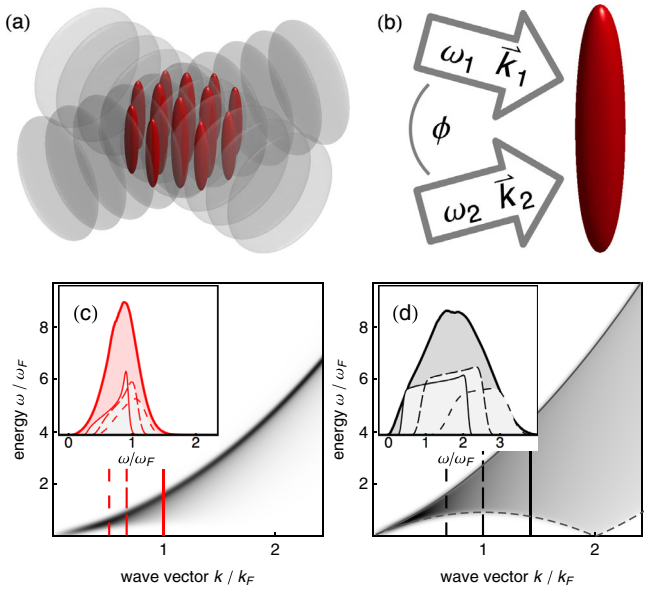

FIG. 1 (color online). Sketch of the experimental setup. (a) A pair of retro-reflected laser beams creates an ensemble of ≈4000 independent one-dimensional Bose gases. (b) The excitation spectrum is probed by illuminating the gas with a pair of Bragg laser beams. (c)–(d) Zero-temperature dynamical structure factor $S(k,\omega)$ (value shown in gray scale) for a moderately ($\gamma = 3.3$) (c) and a strongly ($\gamma = 45$) (d) interacting homogeneous gas. The solid (dashed) line in (d) shows the dispersion of the Lieb-I (Lieb-II) mode. Insets indicate averaging over an ensemble of trapped systems. The thin lines show fixed momentum cuts at representative densities. The corresponding values for k/k_F are indicated as vertical lines in the $k-\omega$ plane. The thick line shows the averaged response $S(\omega)$ in a local density approximation.

loading, the scattering length a_s is set to $a_s = 173(5)a_0$ via a broad Feshbach resonance [23]. In the deep lattice we then ramp a_s within 50 ms to the desired value in the range $10a_0 \lesssim a_s \lesssim 900a_0$ to prepare the tubes close to the adiabatic ground state. The ramp of a_s is carefully adapted to avoid any excitation of breathing modes.

The gas in each tube is described by the Lieb-Liniger Hamiltonian [16]

$$\hat{H} = -\frac{\hbar^2}{2m}\sum_i \partial^2/\partial z_i{}^2 + g_{1D}\sum_{\langle i,j\rangle}\delta(z_i - z_j), \qquad (1)$$

with $g_{1D} = 2\hbar\omega_\perp a_s(1 - 1.0326a_s/a_\perp)^{-1}$ the coupling strength in one dimension [11,13,24] and $a_\perp = \sqrt{\hbar/(m\omega_\perp)}$ the transverse harmonic oscillator length. The Lieb-Liniger parameter is then defined as $\gamma = mg_{1D}/(\hbar^2 n_{1D})$, where n_{1D} denotes the one-dimensional line density [9]. The density sets the characteristic Fermi wave vector $k_F = \pi n_{1D}$ of the system. In our experimental setup we have to consider two sources of inhomogeneity. First, the tubes are harmonically confined along the longitudinal direction with a trap frequency $\omega_z = 2\pi \times 15.8(0.1)$ Hz. This gives rise to an inhomogeneous density distribution in each quantum wire. Second, the loading procedure leads to a distribution of the number of atoms across the ensemble of 1D systems [23]. For comparing measurements with theoretical predictions, both effects can be accounted for by averaging over homogeneous subsystems in a local density approximation (LDA) [see insets to Figs. 1(c) and (d)].

We probe the spectrum of elementary excitations via two-photon Bragg spectroscopy [25]. In brief, the sample is illuminated for 5 ms with a pair of phase coherent laser beams at a wavelength $\lambda_B \approx 852$ nm and detuned by ≈200 GHz from the Cs $D2$ line. The beams intersect at an angle ϕ at the position of the atoms and are aligned such that the wave vector difference points along the direction of the tubes [Fig. 1(b)]. Its magnitude $k = 4\pi/\lambda_B \sin(\phi/2)$ sets the momentum transfer, while a small frequency detuning ω between the laser beams defines the energy transfer to the system. In linear response, the energy absorbed from the Bragg lasers for a fixed pulse area $\Delta E(k,\omega)$ directly relates to the dynamical structure factor $S(k,\omega) = \int dx \int dt e^{i\omega t - ikx}\langle\rho(x,t)\rho(0,0)\rangle$ at finite temperature T via $\Delta E(k,\omega) \propto \hbar\omega(1 - e^{-\hbar\omega/(k_B T)})S(k,\omega)$ with Boltzmann's constant k_B [26].

In our experiment, we probe the ensemble of 1D tubes at a fixed $k = 3.24(3)$ μm^{-1}, which is comparable to typical mean values for k_F averaged over the sample [27]. The absorbed energy as a function of ω is measured in momentum space. For this, we switch off the lattice potential quickly (within 300 μs) and allow for 50 ms time of flight at a small positive scattering length of ≈$15a_0$. From the integrated line density along the z direction of the tubes we extract $\langle p^2\rangle$ and plot it as a function of ω. The result for five different values of γ is depicted in Figs. 2(a)–2(e).

The data sets cover the regime from weak to strong interactions $0.1 \lesssim \gamma \lesssim 50$ probed at $0.3 \lesssim k/k_F \lesssim 1$. The variation in k/k_F ensues from the change of the density distribution in the tubes with increasing a_s, evolving from a Thomas-Fermi profile at weak interactions towards the TG profile at strong interactions. The values for γ and k_F given in Fig. 2 denote the average over the ensemble of 1D systems, using the mean n_{1D} in each wire calculated for $T = 0$ from the solution of the Lieb-Liniger integral equations in LDA [23]. Error bars reflect mainly a ±10% uncertainty in the total atom number. A clear interaction-induced broadening and shift of the spectra with increasing γ is observed in accordance with the calculated position of the Lieb-I and Lieb-II modes (vertical dashed lines) [17]. We compare the data set in the strongly interacting regime [Fig. 2(e)] to the calculated response for an ensemble of trapped TG gases at zero temperature averaged over the ensemble of tubes (dashed line) [23,28]. The agreement with the data underlines the contribution of Lieb's holelike excitation to the dynamical response.

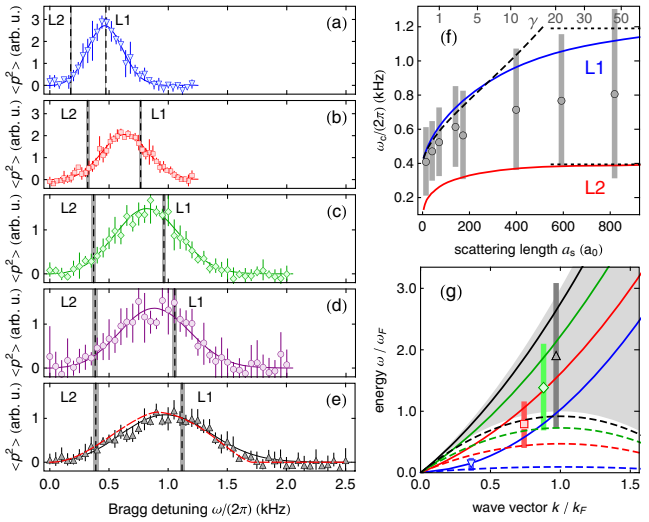

FIG. 2 (color online). Bragg-excitation spectra for different values of the 1D interaction strength γ. (a)–(e) Transferred energy $\sim\langle p^2\rangle$ (normalized to unit area) as a function of the Bragg detuning ω. The scattering length is set to $15a_0$ (a), $173a_0$ (b), $399a_0$ (c), $592a_0$ (d), and $819a_0$ (e), giving an average $\gamma[k_F/\mu\mathrm{m}^{-1}]$ of 0.12(5) [9(1)], 3.3(1) [4.4(2)], 11.0(4) [3.7(1)], 21.7(7) [3.5(1)], and 45(1) [3.3(1)], respectively. Solid lines show fits to the data using a Gaussian multiplied by ω. The vertical dashed lines indicate the position of the Lieb-I (L1) and Lieb-II (L2) mode calculated with the averaged values for γ [23]. The dashed line in (e) shows the calculated response for ensemble-averaged trapped TG gases. (f) Central excitation energy ω_c extracted from the Gaussian fit model as a function of a_s (circles). Solid (dashed) lines denote the calculated position of the Lieb-I or -II modes (Bogoliubov mode). The dotted lines indicate the energy of particle and hole excitations in the TG limit. (g) ω_c extracted from the data shown in (a) (triangle), (b) (square), (c) (diamond), and (e) (inverted triangle) plotted in the dimensionless energy-momentum plane. Solid (dashed) lines denote the Lieb-I (Lieb-II) mode. The shaded area shows the continuum of excitations in the TG limit. Vertical lines in (f) and (g) give the fitted full width at half maximum (FWHM).

Prior to a detailed discussion on the exact line shape for finite γ and finite T, we attempt a simplified zero-temperature analysis of our spectroscopy signal. A function $\propto \omega\mathcal{G}(\omega_c)$ is fit to the data (solid lines), where the DSF averaged over the ensemble of tubes is approximated by a simple Gaussian function $\mathcal{G}$ centered at ω_c. The extracted ω_c as a function of a_s is shown in Fig. 2(f) (circles). The vertical lines denote the fitted FWHM. We find the spectral weight of the data within the Lieb-I and Lieb-II modes (solid lines) calculated using the ensemble-averaged values for γ. Bogoliubov's quasiparticle energy alone (dashed line) does not explain the observed ω_c with increasing $\gamma \gtrsim 3$. We summarize the measured spectral position and width for four selected values of γ in the dimensionless energy-momentum plane in Fig. 2(g), with $\omega_F = \epsilon_F/\hbar = \hbar k_F^2/(2m)$. Comparing this to the dispersion relation of Lieb's particle and holelike excitation, we observe a clear signature for the contribution of both branches with increasing interactions, finally approaching the limit of the excitation spectrum of the fully fermionized Bose gas (shaded area).

We now turn to a detailed analysis of the spectral line shape as a function of interaction strength and temperature. The effect of temperature on the measurement of the DSF arises from two distinct contributions. First, the DSF itself is temperature dependent. This becomes most evident in the TG limit of fermionized bosons. For $k_BT \ll \epsilon_F$ the effective Fermi sea in quasimomentum space has a sharp edge, giving rise to a homogeneous continuum of excitations lying between Lieb's hole- and particlelike modes. When $k_BT \sim \epsilon_F$ the Fermi edge washes out; this results in a smoothing of the DSF, with its spectral weight being shifted to higher energies [20]. Second, finite temperature affects the density distribution in our 1D systems, leading to a decreasing mean n_{1D} with increasing T for fixed a_s. This changes the average k/k_F at which the tubes are probed.

For our theoretical analysis we take both effects into account. First, we calculate the density distribution in each of the tubes at a temperature T by numerically solving the Yang-Yang integral equations for the 1D Bose gas [29]. The DSF is evaluated at finite T via the ABACUS algorithm, a Bethe ansatz-based method to compute correlation functions of integrable models [30]. The effect of the trapping potential is incorporated by making a LDA for each tube. The response of the array of tubes is finally calculated by weighting the contribution of each subsystem by the number of atoms [23].

The result of our theoretical analysis for four different values of γ is presented in Fig. 3 and is compared to the corresponding experimental data [taken from Figs. 2(b)–2(e)]. Although finite temperature leads to small shifts and broadening of the excitation spectrum, the most relevant contribution to the spectral shape stems from the broadening of the dynamical structure factor with increasing interactions. The analysis underlines the contribution of holelike excitations to the overall response when entering deep into the strongly correlated regime. Further, a reduced χ^2 analysis of our data with the computed spectra serves as a thermometry tool in the tubes and points to gas temperatures in the range of 5 to 10 nK. A moderate increase in temperature is seen for increasing values of γ [23].

So far, we have characterized the excitations in the gas by measuring $\langle p^2\rangle$. Now, we analyze the full momentum distribution $n(p)$ of the excited 1D Bose gases. In Figs. 4(a)–4(c) we plot the atomic line density after time of flight, integrated transversally to the direction of the tubes, which reflects the in-trap momentum distribution of the atomic ensemble. The measurements are taken at three different values of γ, ranging from the weakly to the strongly interacting regime, and at Bragg excitation frequencies ω slightly below (left column), just at (central column), and slightly above (right column) the peak of the resonance.

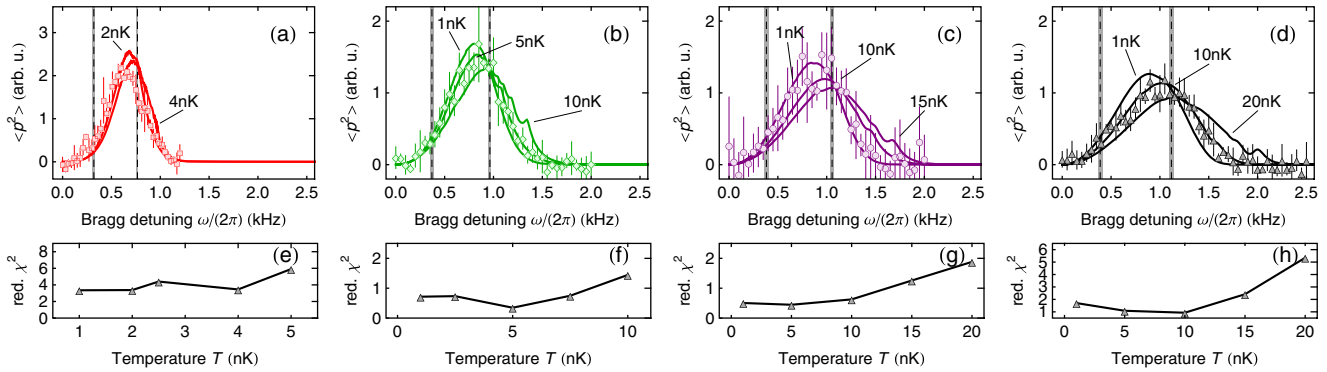

FIG. 3 (color online). Comparison of the Bragg-excitation spectra with theoretical predictions at finite temperature. Symbols depict the data presented in Fig. 2 for $\gamma = 3.3(1)$ (a), $\gamma = 11.0(4)$ (b), $\gamma = 21.7(7)$ (c), and $\gamma = 45(1)$ (d). The vertical dashed lines indicate the position of the Lieb-I and Lieb-II modes calculated with the averaged values for γ. The solid lines show the ensemble-averaged response derived from the finite temperature dynamical structure factor. (e)–(h) Reduced χ^2 analysis of the corresponding experimental data in the top row with theoretical predictions for different temperatures.

First, we recognize a dramatic qualitative change in $n(p)$ with increasing γ for all detunings presented. In the weakly interacting regime [Fig. 4(a)], we observe a clear particlelike excitation located at $p = \hbar k$, as expected from the noninteracting limit. However, with increasing interactions this feature smears out and evolves towards an overall broadening of $n(p)$, indicative of a strong collective response of the system to the Bragg pulse. This observation demonstrates one of the key features of 1D systems: any excitation to the system is necessarily collective, and, therefore, leads to energy-broadened response functions, in contrast to sharp coherent single-particle modes. This broadening, however, only becomes clearly visible for strong-enough interactions, where the holelike modes become dynamically relevant.

In a further measurement, we attempt to quantify the response in momentum space in more detail. Note that our previous measurement of $\langle p^2 \rangle$ captures both a broadening of the momentum distribution as well as an increase in the mean momentum $\langle p \rangle$. In order to separate both contributions spectroscopically, we plot the relative change δw of the width w of the central part of $n(p)$ around $p = 0$ and $\langle p \rangle$ as a function of ω for different values of γ in Figs. 4(d)–4(f). The data indicate how collective excitations in the gas, expressed via energy deposition in w rather than in $\langle p \rangle$, become dominant with increasing γ. Interestingly, the two curves peak at different values for ω. This observation is confirmed by the momentum-space character of elementary excitations in the interacting 1D systems, which changes from a collective broadening for the Lieb-II mode to a particlelike feature for the Lieb-I mode with increasing ω [23].

In conclusion, we have measured the excitation spectrum of a strongly correlated 1D system for a wide range of interaction parameters. Comparison with integrability-based calculations at finite temperature allows for a direct observation of the contribution of the collective Lieb-II mode to the DSF. Our results demonstrate the successful application of an integrable model to analyze dynamics of the 1D Bose gas. Furthermore, the collective nature of elementary excitations in one dimension with increasing

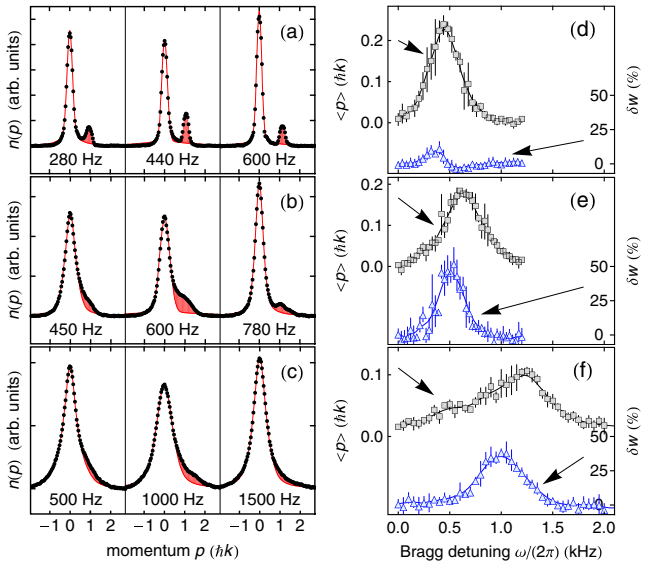

FIG. 4 (color online). Momentum distribution $n(p)$ for resonant and off-resonant Bragg excitation measured at weak and strong interactions. (a)–(c) Integrated line density after 50 ms time of flight when exciting the 1D systems at $\gamma = 0.12(5)$ (a), $\gamma = 3.3(1)$ (b), and $\gamma = 45(1)$ (c) for red-detuned (left), resonant (middle), and blue-detuned (right) excitation with respect to the Bragg resonance. Data points show the average of four measurements. The frequencies given denote the Bragg detuning $\omega/(2\pi)$. The red line shows a fit to the central part of the line density around $p = 0$, using a linear combination of a Lorentzian and Gaussian profile to extract the width w. The red shaded area denotes the fraction of atoms asymmetrically scattered to higher momentum states. (d)–(f) Imparted mean momentum $\langle p \rangle$ extracted from $n(p)$ (squares) and relative change in the fitted width δw of the central peak around $p = 0$ (triangles) as a function of the detuning $\omega/(2\pi)$ for $\gamma = 0.12(5)$ (d), $\gamma = 3.3(1)$ (e), and $\gamma = 45(1)$ (f). Solid lines are interpolating functions to guide the eye.

interaction strength has been demonstrated through an analysis of the momentum distribution. Our results pose questions on the time evolution and potential equilibration of these collective excitations. This could be seen as an alternative quantum cradle setting [31] in which, instead of colliding two highly energetic clouds of atoms, relatively low-energy excitations propagate through the system, and their individual features can then be more easily studied.

We are indebted to R. Grimm for generous support, and we thank M. Buchhold and S. Diehl for fruitful discussions. We gratefully acknowledge funding by the European Research Council (ERC) under Project No. 278417 and under the Starting Grant No. 279391 EDEQS, by the Austrian Science Foundation (FWF) under Project No. P1789-N20, and from the FOM and NWO foundations of the Netherlands.

[1] T. Giamarchi, *Quantum Physics in One Dimension* (Oxford University Press, New York, 2004).
[2] O. M. Auslaender, A. Yacoby, R. de Picciotto, K. W. Baldwin, L. N. Pfeiffer, and K. W. West, Science **295**, 825 (2002).
[3] G. Barak, H. Steinberg, L. N. Pfeiffer, K. W. West, L. Glazman, F. von Oppen, and A. Yacoby, Nat. Phys. **6**, 489 (2010).
[4] F. D. M. Haldane, Phys. Rev. Lett. **47**, 1840 (1981).
[5] A. Imambekov and L. I. Glazman, Science **323**, 228 (2009).
[6] A. Imambekov, T. L. Schmidt, and L. I. Glazman, Rev. Mod. Phys. **84**, 1253 (2012).
[7] M. Mourigal, M. Enderle, A. Klöpperpieper, J.-S. Caux, A. Stunault, and H. M. Rønnow, Nat. Phys. **9**, 435 (2013).
[8] B. Lake, D. A. Tennant, J.-S. Caux, T. Barthel, U. Schollwöck, S. E. Nagler, and C. D. Frost, Phys. Rev. Lett. **111**, 137205 (2013).
[9] M. A. Cazalilla, R. Citro, T. Giamarchi, E. Orignac, and M. Rigol, Rev. Mod. Phys. **83**, 1405 (2011).
[10] T. Kinoshita, T. Wenger, and D. S. Weiss, Science **305**, 1125 (2004).
[11] E. Haller, M. Gustavsson, M. J. Mark, J. G. Danzl, R. Hart, G. Pupillo, and H.-C. Nägerl, Science **325**, 1224 (2009).
[12] M. Girardeau, J. Math. Phys. (N.Y.) **1**, 516 (1960).
[13] E. Haller, M. J. Mark, R. Hart, J. G. Danzl, L. Reichsöllner, V. Melezhik, P. Schmelcher, and H.-C. Nägerl, Phys. Rev. Lett. **104**, 153203 (2010).
[14] E. Haller, M. Rabie, M. J. Mark, J. G. Danzl, R. Hart, K. Lauber, G. Pupillo, and H.-C. Nägerl, Phys. Rev. Lett. **107**, 230404 (2011).
[15] N. Fabbri, M. Panfil, D. Clément, L. Fallani, M. Inguscio, C. Fort, and J.-S. Caux, Phys. Rev. A **91**, 043617 (2015).
[16] E. H. Lieb and W. Liniger, Phys. Rev. **130**, 1605 (1963).
[17] E. H. Lieb, Phys. Rev. **130**, 1616 (1963).
[18] J.-S. Caux and P. Calabrese, Phys. Rev. A **74**, 031605(R) (2006).
[19] A. Y. Cherny and J. Brand, Phys. Rev. A **73**, 023612 (2006).
[20] M. Panfil and J.-S. Caux, Phys. Rev. A **89**, 033605 (2014).
[21] T. Weber, J. Herbig, M. Mark, H.-C. Nägerl, and R. Grimm, Science **299**, 232 (2002).
[22] T. Kraemer, J. Herbig, M. Mark, T. Weber, C. Chin, H.-C. Nägerl, and R. Grimm, Appl. Phys. B **79**, 1013 (2004).
[23] See Supplemental Material at http://link.aps.org/supplemental/10.1103/PhysRevLett.115.085301 for details on the calculation of mean density, interaction strength and Fermi wave-vector in the tubes, the sampling of the DSF, the ABACUS algorithm, and for a discussion on the regime of linear response, heating effects, and the spectral width at weak interactions.
[24] M. Olshanii, Phys. Rev. Lett. **81**, 938 (1998).
[25] J. Stenger, S. Inouye, A. P. Chikkatur, D. M. Stamper-Kurn, D. E. Pritchard, and W. Ketterle, Phys. Rev. Lett. **82**, 4569 (1999).
[26] A. Brunello, F. Dalfovo, L. Pitaevskii, S. Stringari, and F. Zambelli, Phys. Rev. A **64**, 063614 (2001).
[27] We calibrate k from the measured Bragg excitation spectrum of a weakly interacting BEC in three dimensions.
[28] V. N. Golovach, A. Minguzzi, and L. I. Glazman, Phys. Rev. A **80**, 043611 (2009).
[29] C. N. Yang and C. P. Yang, J. Math. Phys. (N.Y.) **10**, 1115 (1969).
[30] J.-S. Caux, J. Math. Phys. (N.Y.) **50**, 095214 (2009).
[31] T. Kinoshita, T. Wenger, and D. S. Weiss, Nature (London) **440**, 900 (2006).